Article

Not peer-reviewed version

# Enhanced Tribological and Electrical Performance of Graphene-Coated Polyetheretherketone Nanocomposites

Pyoung-Chan Lee , Seo-Hwa Hong , Jung Hoon Kim , Jae Young Seo , Youn Ki Ko , Jin Uk Ha , Sun Kyoung Jeoung , Myeong-Gi Kim * , Beom-Gon Cho *

Posted Date: 4 February 2025

doi: 10.20944/preprints202502.0159.v1

Keywords: Polyetheretherketone (PEEK); Chemical modified graphene (CMG); Nanocomposites; Friction; Electric Resistance

*Article*

# Enhanced Tribological and Electrical Performance of Graphene-Coated Polyetheretherketone Nanocomposites

**Pyoung-Chan Lee [1], Seo-Hwa Hong [1], Jung Hoon Kim [2], Jae Young Seo [2], Youn Ki Ko [1], Jin Uk Ha [1], Sun Kyoung Jeoung [1], Myeong-Gi Kim [2,*] and Beom-Gon Cho [3,*]**

[1] Chassis & Materials Research Laboratory, Korea Automotive Technology Institute, 303 Pungse-ro, Pungse-myeon, Dongnam-gu, Cheonan-si, Chungcheongnam-do 31214, Republic of Korea; pclee@katech.re.kr (P.-C.L.); shhong1@katech.re.kr (S.H.H); ykko@katech.re.kr (Y.K.K.); juha@katech.re.kr (J.U.H.); skjeong@katech.re.kr (S.K.J.)

[2] R&D Center, BESTGRAPHENE Co., Ltd., Yeoju-si, Gyeonggi-do 12616, Republic of Korea; run8827@best-graphene.com (J.H.K.); jyseo@best-graphene.com (J.Y.S.)

[3] Department of Polymer Science and Engineering, Kumoh National Institute of Technology, 61 Daehak-ro, Gumi, Gyeongbuk 39177, Republic of Korea

* Correspondence: mgkim@best-graphene.com (M.-G.K.); bgcho@kumoh.ac.kr (B.-G.C.); Tel.: +82-31-883+8858 (M.-G.K.); +82-54-478-7684 (B.-G.C.)

**Abstract:** Polyetheretherketone (PEEK) is widely used across various industries because of its high thermal stability, chemical resistance, and superior mechanical properties. This paper introduces an optimized method for dispersing functionalized graphene to improve the frictional and electrical resistance properties of PEEK. The influence of graphene, recognized as an effective additive, on the melt behavior, thermal stability, and tribological and electrical properties of PEEK–graphene nanocomposites was assessed for different filler contents. Results show that graphene acts as a nucleating agent, enhancing crystallinity in PEEK–graphene nanocomposites. A nanocomposite containing 1.0 wt.% graphene exhibited optimal frictional performance and surface resistance. Additionally, the study reveals that the integration of hybrid additives with varied shapes fosters the formation of three-dimensional particle networks more effectively than graphene additives alone.

**Keywords:** Polyetheretherketone (PEEK); Chemical modified graphene (CMG); Nanocomposites; Friction; Electric Resistance

## 1. Introduction

Polyetheretherketone (PEEK) is a high-performance engineered polymer with excellent thermal stability, chemical resistance, and mechanical properties. These characteristics are attributed to its aromatic structure and semi-crystalline nature, which are influenced by its thermomechanical processing history. Owing to its durability and high-temperature resistance, PEEK is widely used in automotive, medical, and aerospace industries as a substitute for metal components [1–16].

In industrial production, semi-finished products, including sheets, blocks, and rods, are manufactured in pre-final stages. Several polymer-based semi-finished products are fiber-reinforced plastics (FRPs) with thermoset matrices such as epoxy and unsaturated polyester, typically produced by pultrusion. When high mechanical strength is unnecessary, thermoplastic-based semi-finished products such as PEEK are often preferred. The chemical resistance and dimensional stability of PEEK make it well-suited for semiconductor and display components, where dimensional precision is essential. For insulating polymer components, maintaining a surface resistance between $10^4$ and $10^8$ ohms/sq can mitigate static electricity. To achieve this, conductive additives such as carbon black, carbon fibers, carbon nanotubes, and graphene are commonly added to composites [17–19].

 doi:10.20944/preprints202502.0159.v1



Various fillers are added to polymer matrices to enhance their properties, significantly affecting their mechanical, chemical, electrical, thermal, and tribological performances. The effect of fillers on these properties depends on factors such as composition, shape, and size. Common strategies for improving PEEK include the addition of carbon-based fillers [4–6], ceramic fillers [7,8], glass and carbon fibers [9–12], and solid lubricants [13,14]. Studies have shown that nanoscale fillers improve wear resistance and mechanical properties, with the filler shape playing an essential role in frictional behavior [2].

Graphene, a two-dimensional monolayer of graphite, has attracted attention as a filler for its outstanding electrical, mechanical, wear-resistant, and thermal properties. Owing to its high elastic modulus and tensile strength, graphene enhances the stiffness and mechanical integrity of composites [1,15,16,20–22]. Its large surface area provides a broad interface to polymer matrices, which improves load transfer and overall composite strength. Furthermore, graphene's two-dimensional structure can function as a lubricant additive, solid lubricant, or sliding coating [1,20–27]. Previous studies have investigated how graphene fillers affect the thermal stability and tribological and mechanical properties of polymers, such as polyamide 6 [25], polyamide 46 [20], polyacrylonitrile [26], polyimide [27], and PEEK [1,2,21,22]. Puértolas et al. [1] developed PEEK–graphene nanoplatelets (GnPs) through solvent-free melt-blending and injection molding. Compared to conventional PEEK, these nanocomposites demonstrated enhanced surface hardness and a lower friction coefficient. However, the high concentration of GnPs required (1–10 wt.%) and the challenges of achieving uniform dispersion through melt blending alone limited the full benefits of graphene [20].

In this study, we developed an efficient method to uniformly disperse graphene to enhance the tribological and electrical properties of PEEK. PEEK–graphene nanocomposites were prepared through controlled interactions between chemically modified graphene (CMG) and PEEK. CMG was designed to promote chemical interactions with polar groups of PEEK. We analyzed the effects of graphene content on the melting behavior, friction, and electrical properties of PEEK–graphene nanocomposites with the goal of enhancing the performance while ensuring uniform dispersion.

## 2. Materials and Methods

### *2.1. Materials*

Ultrafine PEEK powder (880UFP grade) was sourced from Solvay Co. (Brussels, Belgium). Graphite flakes, with a thickness of 150 μm and specifically designed for graphene applications, were obtained from Graphene Supermarket (Ronkonkoma, NY, USA). Chemicals including 4,4-oxydianiline (>97%, Sigma-Aldrich, St. Louis, MO, USA), N,N-dimethylformamide (DMF, >99.5%, TCI, Tokyo, Japan), acetone (>99.5%, TCI, Tokyo, Japan), and 1-methyl-2-pyrrolidinone (NMP, >99%, TCI, Tokyo, Japan) were used without additional pre-treatment. Expanded graphite (ES 100, Samjungcng Co., Gyeongsan-si, Korea) was used to produce graphene nanoplatelets (GnPs).

### *2.2. Preparation of Nanofiller*

The CMG was prepared to facilitate molecular-level chemical interactions with PEEK. Accordingly, a graphene oxide (GO) solution containing hydroxyl, carboxyl, and epoxide groups was prepared to fabricate the CMG as outlined in previous studies [15,28,29].

A graphene surface modification reaction was conducted using 4,4-oxydianiline to obtain CMG colloids capable of interacting with PEEK [20,29]. A solution of 0.1% of GO (500 mL) was prepared via ultrasonication for at least 2 h. Subsequently, 4,4-oxydianiline (20 g) was added to 500 mL of DMF, and the mixture was stirred at 90 °C for 40 h. The reaction product was cooled to 20–25 °C and then subjected to centrifugation to obtain the precipitate. The precipitate was washed three to five times with acetone and filtered. The resulting graphene layers were immediately placed in an ethanol bath. The electrostatic repulsion between the positive charges of 4,4-oxydianiline ($–N^+$) and the graphene

 doi:10.20944/preprints202502.0159.v1



monolayer results in a highly dispersive functionalized graphene colloid with a positive charge ($CMG^+$). The graphene content was adjusted to 1 wt.% by controlling the amount of solvent.

The GnPs were fabricated by liquid exfoliation as follows: The NMP solution was ball-milled at 50 rpm for 24 h with 10 wt.% expanded graphite (ES 100 grade) for expansion treatment. Subsequently, the samples were subjected to primary pulverization and homogenization using a homogenizer (15000 rpm, 1 h), followed by high-pressure homogenization at 1500 bar for 10 passes. Finally, a 10 wt.% GnP with NMP dispersion was prepared by passing the sample through a 100 μm filter in a pressure filtration system and homogenizing with a homogenizer.

### *2.3. Preparation of Nanocomposites*

As shown in Figure 1, in step 1, the PEEK powder was mixed with 1.0 wt.% $CMG^+$ colloid. The graphene content was set to 0.1, 0.3, and 0.5 wt.%. The mixture was subjected to high-speed revolution and rotation using a Thinky mixer at revolution and rotation speeds of 2000 and 800 rpm, respectively, with each cycle lasting 3 min. This process was repeated three times. The samples produced using 0.1, 0.3, and 0.5 wt.% graphene were named CMG0.1, CMG0.3, and CMG0.5, respectively. In step 2, PEEK–graphene powder with a PEEK(core)–CMG(shell) structure was fabricated by drying the as-prepared samples in a vacuum oven at 60 °C for 12 h. Steps 1 and 2 were conducted once to produce CMG0.5. CMG1.0 and CMG2.0 were manufactured by repeating steps 1 and 2 two or four times, respectively. The hybrid sample CMG1.0/GnP1.0 was prepared by adding 10 g of a 10 wt.% GnP with NMP dispersion to 100 g of CMG1.0 powder. The mixture was then subjected to high-speed revolution and rotation mixing using a Thinky mixer at revolution and rotation speeds of 2000 and 800 rpm, respectively, for 3 min. The cycles were repeated three times. Finally, the CMG1.0/GnP1.0 sample was obtained by drying the product in a vacuum oven at 120 °C for 12 h. To analyze the properties of PEEK–graphene powder, specimens were fabricated via hot press (Qmesys, Uiwang-si, South Korea). After placing the powder into a mold, it was subjected to a pressure of 5 bar for 30 min at a temperature of 380 °C.

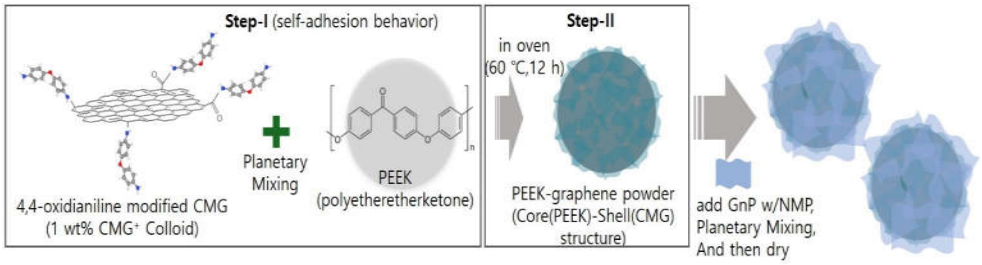


**Figure 1.** Schematic of PEEK-Graphene nanohybrid material fabrication.

### *2.4. Characterization*

Elemental analysis (EA, FlashSmart, Thermo Fisher Scientific, Waltham, MA, USA) was conducted to examine the chemical modifications of GO and graphene. The morphologies of $CMG^+$ and GnPs were analyzed using atomic force microscopy (AFM, FX40, Park Systems, Suwon-si, Republic of Korea) and scanning electron microscopy (SEM, VEGA, TESCAN, Brno, Czech Republic), respectively. The graphene additives were analyzed using zeta potential measurements (LITESIZER 500, Anton Paar, Graz, Austria) and Raman spectroscopy (Confotec MR350, SOL Instruments, Minsk, Belarus).

The PEEK–graphene powder was analyzed by Raman spectroscopy and SEM. The particle size distributions in pristine PEEK and PEEK–graphene powder were measured using a laser diffraction particle size analyzer (Mastersizer, Malvern Panalytical, Malvern, Worcestershire, U.K.) in the range of 10 nm–3500 μm. The melt flow index (MI) of PEEK–graphene powder was analyzed using a melt flow indexer (MI-2, GöTTFERT, Buchen, Germany) at a temperature of 380 °C and load of 5.2 kg.

 doi:10.20944/preprints202502.0159.v1



The effect of graphene content on crystallization was evaluated using a polarization microscope (VHX-7000, Keyence, Osaka, Japan) in conjunction with a hot stage (LTS420, Linkam Scientific Instruments, Salfords, U.K.). The powder was heated at a rate of 50 °C $min^{-1}$ until 400 °C, after which the temperature was held at 400 °C for 5 min to melt the powder. Subsequently, the sample was cooled at a rate of 10 °C per min until reaching 30 °C, resulting in the formation of crystals. The crystallinity of the PEEK–graphene powder was analyzed via differential scanning calorimetry (DSC, DSC4000, PerkinElmer, Waltham, MA, USA) at a heating rate of 10 °C $min^{-1}$ in the temperature range of 50–400 °C. The DSC measurements were conducted after the samples were sealed in an aluminum pan under a nitrogen atmosphere. The melting temperature ($T_m$) was defined as the temperature corresponding to the maximum endothermic peak observed during the heating scan, whereas the crystallization temperature ($T_c$) was defined as the temperature corresponding to the minimum exothermic peak observed during the cooling scan. The degree of crystallinity of PEEK in the PEEK–graphene nanocomposites, $X_c$, was obtained by dividing the corrected melting enthalpy by the melting enthalpy of a 100% crystalline PEEK (130 J $g^{-1}$) [21]. Thermogravimetric analysis (TGA) was performed using a TGA4000 instrument (Perkin Elmer). The analysis was conducted under a nitrogen atmosphere at a heating rate of 10 °C $min^{-1}$, with a gas flow rate of 20 mL $min^{-1}$.

The friction properties of PEEK–graphene nanocomposites were determined using a pin-on-disc tester (THT, Anton Paar, Graz, Austria). This test was conducted using a 10 N test load at a motor speed of 400 rpm under an ambient temperature of 25 °C. A stainless steel ball with a diameter of 6 mm was used. The surface resistance of the PEEK–graphene nanocomposites was measured using a resistance meter (Trek 152; Advanced Energy, Denver, Colorado, USA).

## 3. Results

### *3.1. Characterization of GnPs and CMG⁺*

EA was used to elucidate the molecular and structural characteristics of the synthesized GnPs and CMG⁺. Table 1 shows the compositions of C, O, and N in GO, CMG⁺, and GnPs. CMG⁺ had C and N contents of 80.10% and 10.05%, respectively, indicating successful functionalization through the reduction of GO and substitution with 4,4-oxydianiline.

**Table 1.** Elemental compositions of GO, CMG⁺, and GnP.

| | C (at.%) | O (at.%) | N (at.%) |
|---|---|---|---|
| GO | 55.37 | 44.63 | 0 |
| CMG⁺ | 80.10 | 9.85 | 10.05 |
| GnP | 99.87 | 0.12 | 0.01 |

The change in the thickness of the CMG⁺ sheet was measured using AFM. Figure 2 shows AFM images and height profiles of the CMG⁺ sheet. The thicknesses of the CMG⁺ sheets varies between 1.45 and 1.34 nm. These values are consistent with the thickness of single-layer graphene on Si wafer substrates.

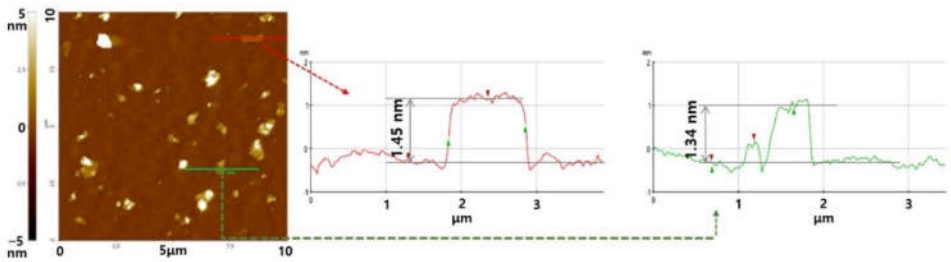


**Figure 2.** AFM non-contact mode image and line profiles of CMG+ on a Si wafer substrate.

 doi:10.20944/preprints202502.0159.v1



Figure S1 shows the SEM micrographs of the GnPs. Compared with CMG+ [20], the GnPs are thicker, possibly owing to slight stacking or agglomeration between the GnP sheets. CMG+ is dispersed as a monolayer in the colloid because of the strong electrostatic repulsion between the graphene sheets [20]. However, the GnPs produced through swelling and mechanical delamination were in the form of flakes with thicknesses of 20–30 nm, indicating graphene sheet stacking.

*3.2. Characterization of PEEK-Graphene Nanocomposites*

3.2.1. Structural and Surface Analysis

Figure 3 shows the zeta potentials of GO, CMG+, GnP, PEEK, and PEEK–graphene nanocomposites. GnP, GO, and CMG exhibit a zeta potential of 0, −34.9, +62.9 mV, respectively. The zeta potential of PEEK is influenced by the presence of ether and ketone groups in its polymer chain and was measured to be −59.2 mV, indicating a highly negative surface charge. These results suggest that PEEK–graphene nanocomposites can be easily and rapidly fabricated using CMG+ owing to the strong electric charge and spontaneous bonding induced by the electrostatic adhesion of the graphene sheets inside the nanocomposites. As shown in Figure 3b, CMG1.0 exhibits a zeta potential of +13.2 mV. This indicated the successful adsorption of CMG+ and PEEK, which have positive and negative surface charges, respectively, onto the PEEK surface via electrostatic forces and ion binding. The hybrid CMG1.0/GnP1.0 sample consisted of GnPs that were physically adsorbed onto the surface of the CMG1.0 powder. This adsorption is induced through van der Waals forces between CMG+ and GnPs, as well as through π-π stacking. Therefore, its zeta potential is close to that of CMG1.0, specifically +15.5 mV. During the injection or extrusion molding of the PEEK–graphene nanocomposite, CMG+ forms a three-dimensional network through ion bonding with the PEEK polymer chain. The GnPs are expected to easily detach from the surface of CMG+ and disperse freely into the graphene sheets inside the nanocomposites.

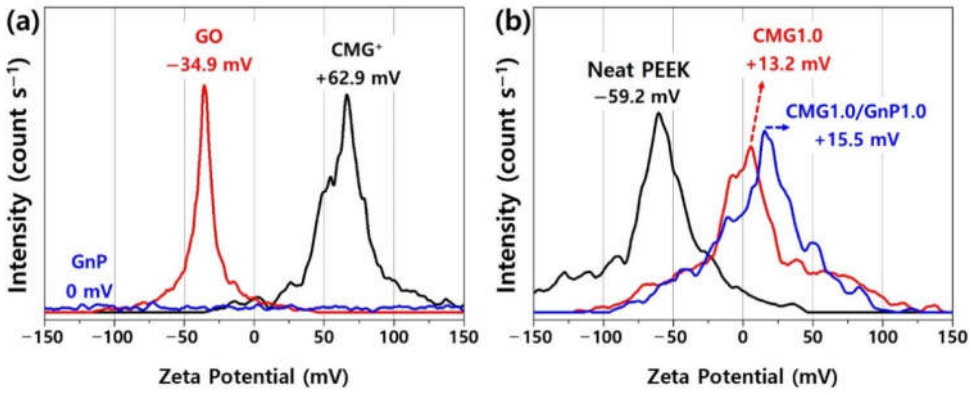


**Figure 3.** Zeta potentials of (a) GO, CMG+, GnP, (b) pristine PEEK, CMG1.0, and CMG1.0/GnP1.0.

The Raman spectra of PEEK exhibit peaks at 1145 $cm^{-1}$ and 1600 $cm^{-1}$, corresponding to the C–O and C=C stretching vibrations, respectively [15,16] (Figure 4). The highly crystalline GnPs exhibit a significantly weak D band at approximately 1360 $cm^{-1}$ but a prominent G band at 1585 $cm^{-1}$. In PEEK–graphene nanocomposites, the presence of CMG+ causes an overlap between the G band of CMG+ at 1585 $cm^{-1}$ and the C=C band of PEEK near 1600 $cm^{-1}$, thereby inducing the formation of broad peaks. The peak broadened with the increasing self-adsorption of CMG+. CMG2.0 does not exhibit the characteristic peaks of PEEK around 1145 and 1600 $cm^{-1}$. This suggests that the bond between the 4,4-oxidianiline group in CMG+ and the oxide group on the surface of the PEEK particles was saturated. CMG1.0/GnP1.0 exhibits a narrower overlapping peak and a shift in the center of the peak toward the G band. This indicates that GnPs were physically well adsorbed onto the surface of the PEEK–graphene.

 doi:10.20944/preprints202502.0159.v1



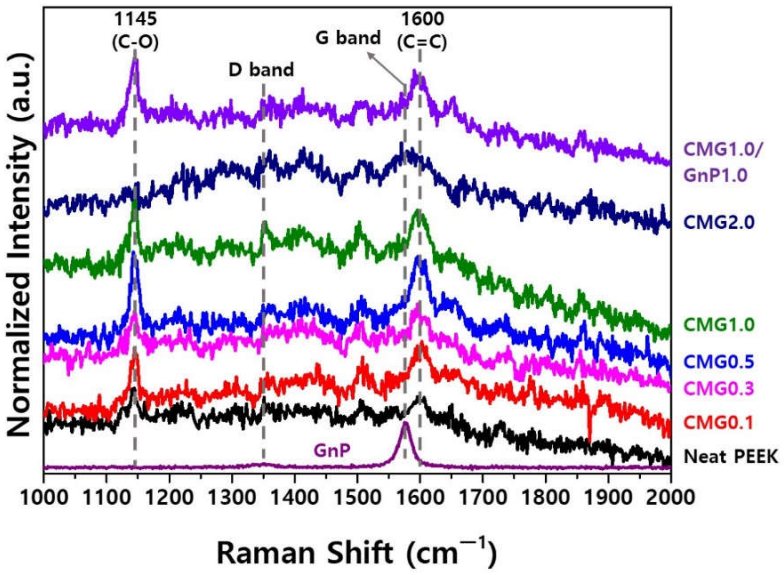


**Figure 4.** Raman spectra of PEEK–graphene nanocomposites for various graphene contents.

Meanwhile, as shown in Figure 5, pristine PEEK powder has a particle size of 20 μm or less. Furthermore, the graphene coating did not cause agglomeration of the PEEK powder. This suggests that the graphene coating does not physically damage the PEEK polymer. High-magnification SEM images confirmed the presence of the graphene coating on the PEEK surface. Figure 6 shows high-magnification (×20,000) SEM images of the images shown in Figure 5. As shown in Figure 6a, the surface of the PEEK powder is smooth. As the graphene content increases, the number of edge shapes (wrinkles and foldings, which are unique morphological features of graphene) on the surface increases. This indicates adsorption of the graphene sheet onto the PEEK surface. This phenomenon becomes more evident as graphene concentration increases. Figure 6f shows the morphology of the CMG sheet with a lateral size of 1–2 μm. As shown in Figure 5g, GnPs do not appear on the external surface of PEEK–graphene particles because they are physically adsorbed onto the CMG layer through van der Waals forces and π-π stacking. Furthermore, as shown in Figure 6g, the surface of the PEEK–graphene particles is enveloped by a thick GnP layer. Therefore, morphological analysis reveals that $CMG^{+}$ in the PEEK–graphene nanocomposite forms a strong three-dimensional network through ion bonding, and GnPs can be easily detached from the surface of PEEK–graphene and dispersed freely into the GnP sheets inside the nanocomposites, supporting the hypothesis of this study.

 doi:10.20944/preprints202502.0159.v1



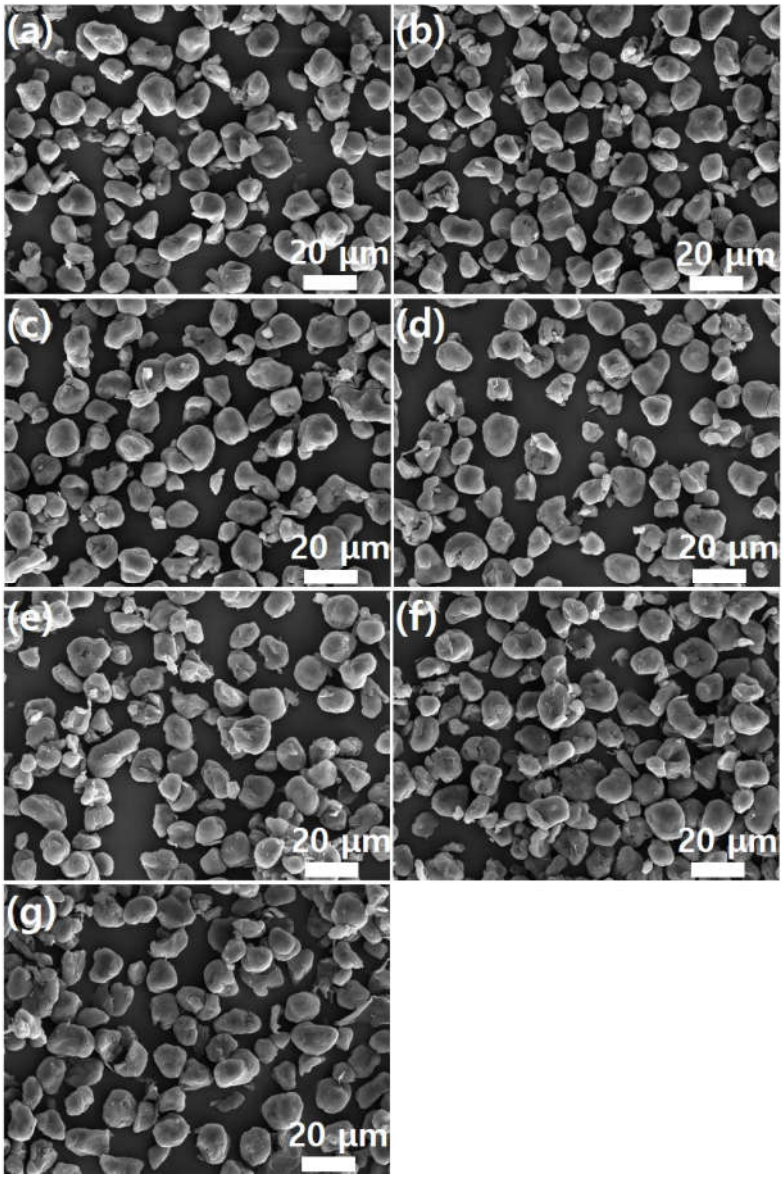


**Figure 5.** SEM images (low magnification) of PEEK–graphene powder for various graphene contents: (a) neat PEEK, (b) CMG0.1, (c) CMG0.3, (d) CMG0.5, (e) CMG1.0, (f) CMG2.0, and (g) CMG1.0/GnP1.0.

 doi:10.20944/preprints202502.0159.v1



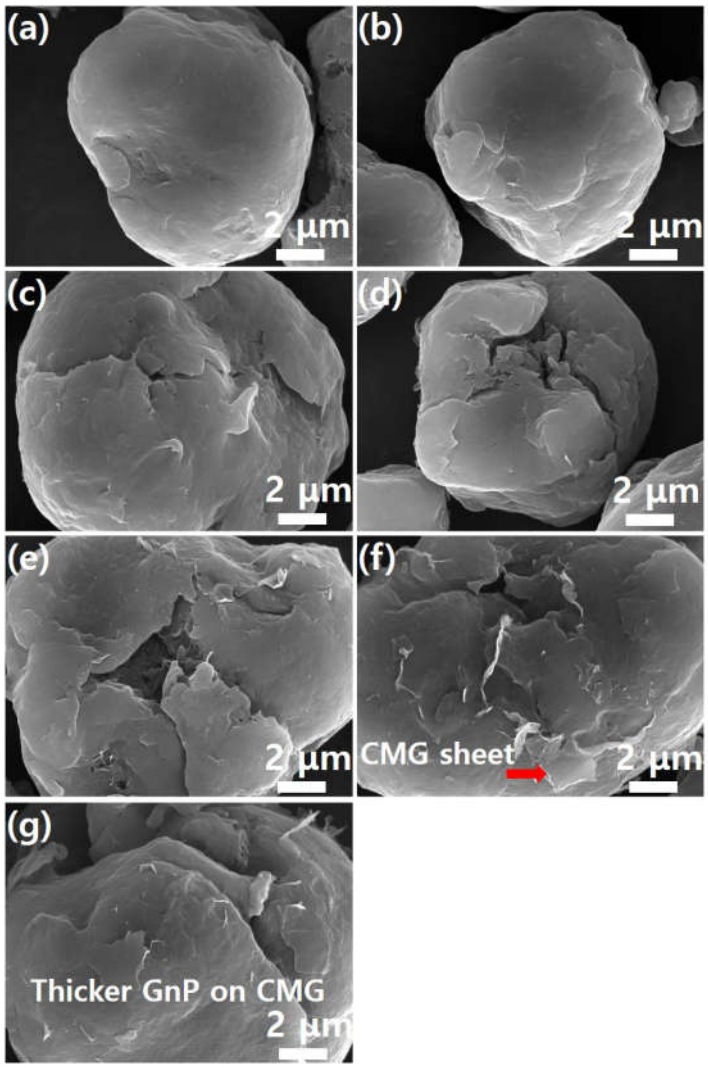


**Figure 6.** SEM images (high magnification) of PEEK–graphene powder for various graphene contents: (a) neat PEEK, (b) CMG0.1, (c) CMG0.3, (d) CMG0.5, (e) CMG1.0, (f) CMG2.0, and (g) CMG1.0/GnP1.0.

Figure 7 shows the particle size distributions of pristine PEEK and PEEK–graphene powders. Pristine PEEK has a uniformly dispersed distribution. When the graphene content is low, the particle distribution appears to be uniform. However, when the graphene content exceeds 1.0 wt.%, particles larger than 100 μm can be observed. In particular, larger particles can be observed at a CMG content of 2.0 wt.%, compared to when the CMG content is 1.0 wt.%. This indicates that an increase in graphene content leads to the partial formation of interparticle networks. Particle size can be measured using various approaches. In this study, the particle size was determined based on the median value. This is defined as the value at which half of the population lies above it and the remaining half lies below it. The median particle size is referred to as $D_v50$. The volume distribution is predominantly determined using laser diffraction, with the quoted baseline D50 representing the volume median. The pristine PEEK exhibits a $D_v50$ of 11.8 μm. PEEK exhibits a $D_v50$ of 11.7–11.8 μm when the CMG content is below 0.5 wt.%. When the CMG content is 1.0 and 2.0 wt.%, it exhibits a $D_v50$ of 12.3 and 13.9 μm, respectively, indicating the generation of larger particles.

 doi:10.20944/preprints202502.0159.v1



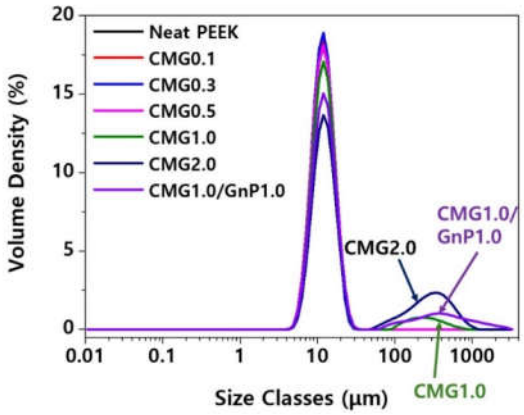


**Figure 7.** Particle size distributions in PEEK–graphene powder for various graphene contents.

3.2.2. Thermal Properties

As shown in Figure 8, the MI decreases with increasing graphene content. Each value represents the average of five measurements. Although error bars are included, the magnitudes of the errors are negligible, making them imperceptible on the graph. Pristine PEEK exhibits an MI of 72.0 g 10 $min^{-1}$, indicating high flowability. In addition, the strand surfaces are smooth. However, when the concentration of graphene increases, the MI decreases in the order 58.1, 63.8, 54.1, 42.8, and 31.4 g 10 $min^{-1}$. However, the surfaces of the strands become rougher as the graphene content increases, along with an increase in the thickness of the strands. CMG1.0/GnP1.0 exhibits an MI of 43.0 g 10 $min^{-1}$, which implies that GnPs have minimal influence on flowability. However, the roughness of the strand surface increased with increasing GnP content, indicating that GnPs have a detrimental effect on the surface quality. The graphene coating layer is predicted to influence the flowability of PEEK–graphene powder. Moreover, graphene is expected to self-adsorb onto the surface of the PEEK powder, forming a core–shell structure (Figure 1). The pristine PEEK melts owing to heat, causing it to merge with the surrounding particles and form a single molten entity. The pristine PEEK melt exhibits high flowability as it is not hindered by obstacles. However, in the case of graphene-coated PEEK powder, the PEEK polymer, after melting, fails to come into contact with the surrounding polymer melt owing to the presence of graphene. This results in the formation of isolated domains that degrade the overall flow. To verify this, the crystallinity was examined using a polarization microscope.

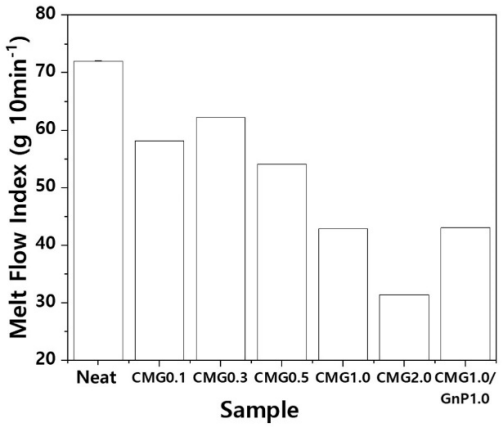


**Figure 8.** MI of PEEK–graphene powders for various graphene contents.

 doi:10.20944/preprints202502.0159.v1



Furthermore, Figure 9 shows the polarization microscopy images for various graphene contents. Figure 9a shows that neat PEEK has a uniform crystalline structure. CMG (0.1) exhibits an area of uneven crystallization (red circle). When the graphene content exceeds 0.3 wt.%, the size of PEEK crystals significantly decreases. Furthermore, a comparison of Figure 9e,g shows that the GnPs do not influence the formation of PEEK crystals. This trend is similar to the melt-flow behavior of the PEEK–graphene powder.

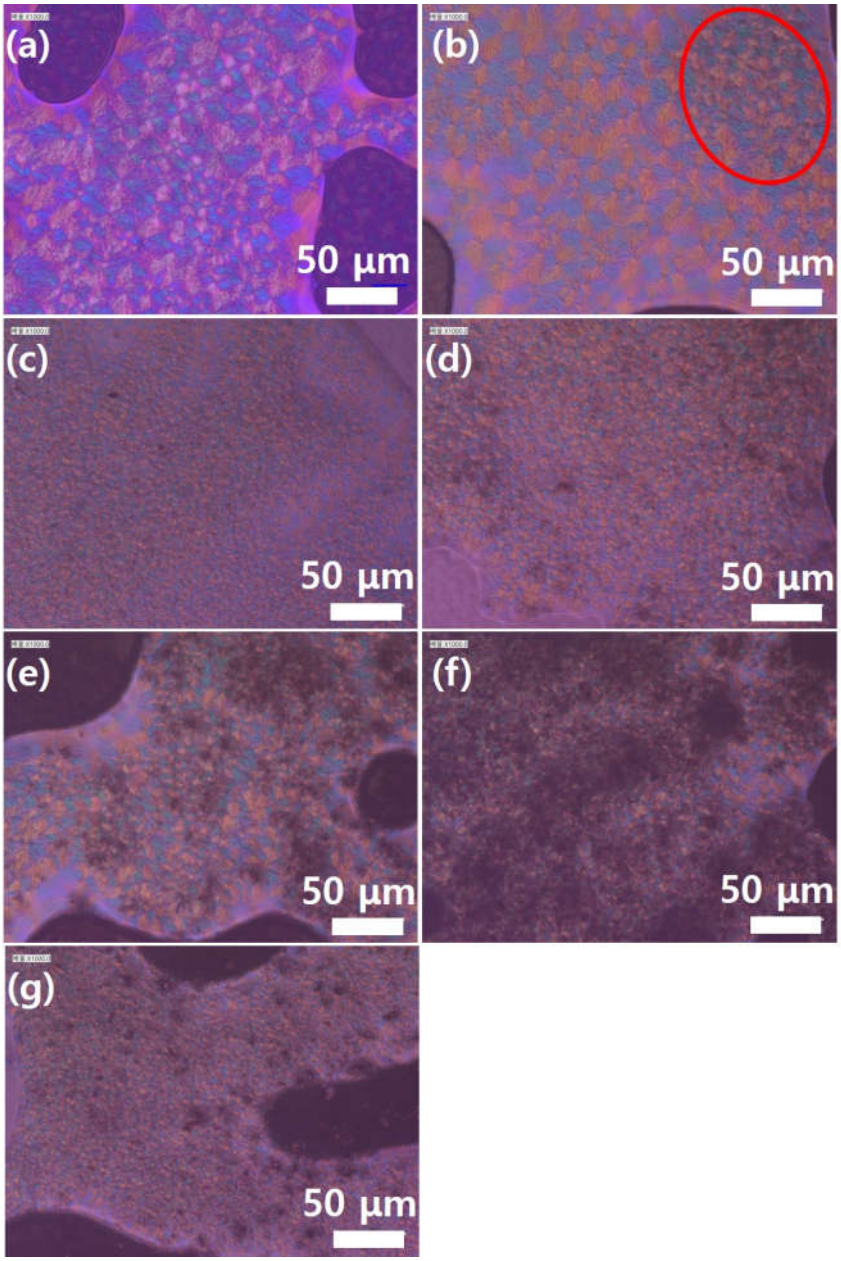


**Figure 9.** Polarization microscope image of PEEK–graphene powder for various graphene contents: (a) neat PEEK, (b) CMG0.1, (c) CMG0.3, (d) CMG0.5, (e) CMG1.0, (f) CMG2.0, and (g) CMG1.0/GnP1.0.

To evaluate the influence of the nanofillers on the crystallization and melting behaviors of the PEEK matrix, a morphological study was conducted by analyzing the nanocomposites using DSC. The degree of crystallinity is known to significantly influence the mechanical properties of polymer materials. The blending of nanofillers can promote either nucleation or confinement, which are two independent effects that influence the crystallization of the polymer matrix. Nanofillers can provide

 doi:10.20944/preprints202502.0159.v1



heterogeneous sites to promote nucleation, thereby increasing the crystallization temperature. However, the formation of a well-developed nanofiller network substantially restricts polymer chain diffusion and crystal growth, delays crystallization, and reduces yield [21]. Figure 10 shows the DSC curves for various graphene contents. The melting points of the nanocomposites are slightly lower than that of pristine PEEK during the heating scan. The lower $T_m$ of the nanocomposites indicates the formation of smaller or less perfect crystals in the nanocomposite. Table S1 lists the values of $T_m$, $T_c$, crystallinity, and $X_c$ obtained from DSC curves. The PEEK–graphene nanocomposites exhibit a higher degree of crystallinity than pure PEEK owing to the nucleating effect of graphene. Therefore, a lower $T_m$ value of the nanocomposite material implies the formation of smaller crystals within it. This phenomenon is consistent with the observations derived from the polarization microscopy images of the samples (Figure 9).

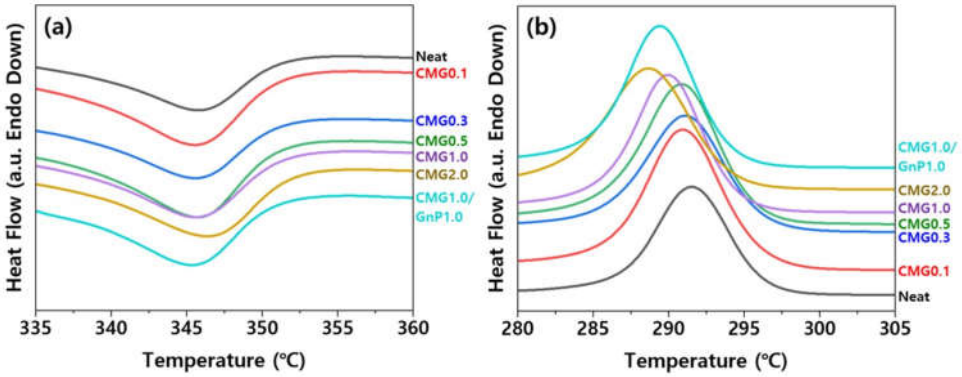


**Figure 10.** Non-isothermal DSC scans (a) heating curves and (b) cooling curves of PEEK–graphene nanocomposites for various graphene contents.

The influence of graphene content on the thermal stability of the PEEK–graphene nanocomposites was analyzed using TGA. As shown in Figure 11, pure PEEK exhibits a single decomposition stage under a nitrogen atmosphere. Decomposition includes decarboxylation and dehydration reactions [21]. The decomposition of pure PEEK begins at 572.6 °C, with the maximum rate observed at 585 °C. The presence of CMG thermally destabilized the nanocomposites, owing to chemical interactions between PEEK and the decomposition products of CMG [21]. As shown in Figure 11, the decomposition of the nanocomposites began at low temperatures. Char residues are formed at temperatures above 800 °C and are composed of carbonized solid residues with distinct aromatic structures. The influence of graphene content on the properties of the PEEK–graphene nanocomposites can be elucidated by examining $T_d$ and $T_{max}$. Graphene acts as a thermal stabilizer in polymers because it hinders the transition of volatile decomposition products from the bulk of the polymer to the gas phase [21,22]. At low concentrations, the presence of graphene does not affect the thermal stability of the nanocomposites. This suggests that the graphene dispersion is insufficient to promote a stabilizing effect. In contrast, the thermal stability of pure PEEK increases slightly when the graphene content exceeds 0.5 wt.%. Notably, the chemical modification of graphene is expected to have two contrasting effects on the thermal stability of composite materials. It enhances the dispersion of the graphene sheet, thereby improving the thermal stability owing to a superior blocking effect. Compared with PEEK, low-molecular-weight functional groups are less thermally stable, consequently reducing the thermal stability of the PEEK composites. Comparison of the performances of CMG1.0/GnP1.0 with those of CMG1.0 and CMG2.0 reveals that GnPs slightly degrade the thermal stability. This implies that CMG1.0 and CMG2.0 exhibit higher thermal stability than the hybrid-type samples.

 doi:10.20944/preprints202502.0159.v1



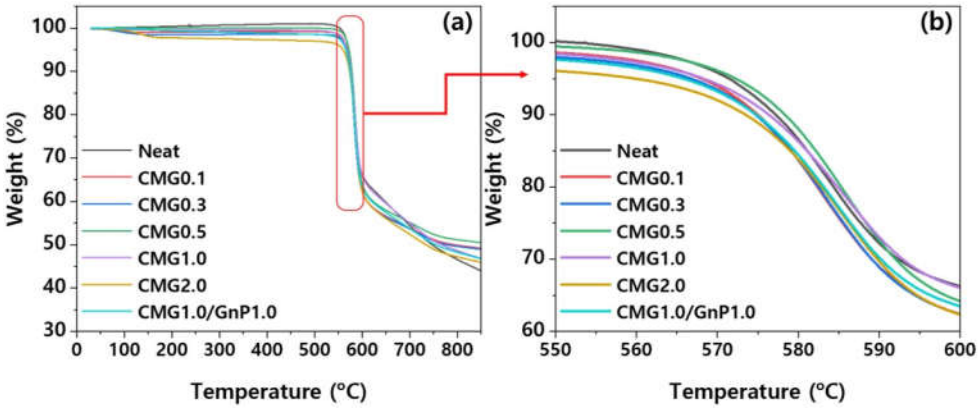


**Figure 11.** (a) Thermogravimetric (TG) curves of PEEK–graphene nanocomposites for various graphene contents and (b) shows magnified view of the thermal degradation region, highlighting the effect of graphene content on the thermal stability and weight loss profile of the PEEK matrix.

### 3.2.3. Tribological Properties

Figure 12 shows the friction coefficients of the PEEK–graphene nanocomposites as a function of graphene content. During the initial stages, the friction coefficient significantly increases owing to the strong frictional forces between the steel ball and the specimen. As the friction continues to increase, the two contact points gradually become slightly smoother, reducing the friction coefficient until it reaches a stable stage. Pristine PEEK has a friction coefficient of approximately 0.35. The friction coefficient gradually decreases with increasing graphene content owing to the two-dimensional structural characteristics of graphene. The friction coefficients of PEEK blended with CMG1.0 and CMG2.0 are approximately 54% and 63% lower than those of pure PEEK, respectively. Furthermore, compared with the CMG2.0 sample, the CMG1.0/GnP1.0 sample exhibits a higher friction coefficient. This can be attributed to the surface roughness of the strands, as observed in the MI measurement results. In the CMG1.0/GnP1.0 samples, the presence of GnPs deteriorates the surface quality and consequently has a negative influence on the friction behavior of the material. Puértolas et al. [1] and Kalin et al. [2] enhanced the friction properties of graphene-based PEEK nanocomposites; however, the graphene content exceeded 1 wt.% and the friction coefficient did not decrease by more than 40%. In this study, the friction coefficient was reduced by more than 50% by using low-loading graphene.

 doi:10.20944/preprints202502.0159.v1



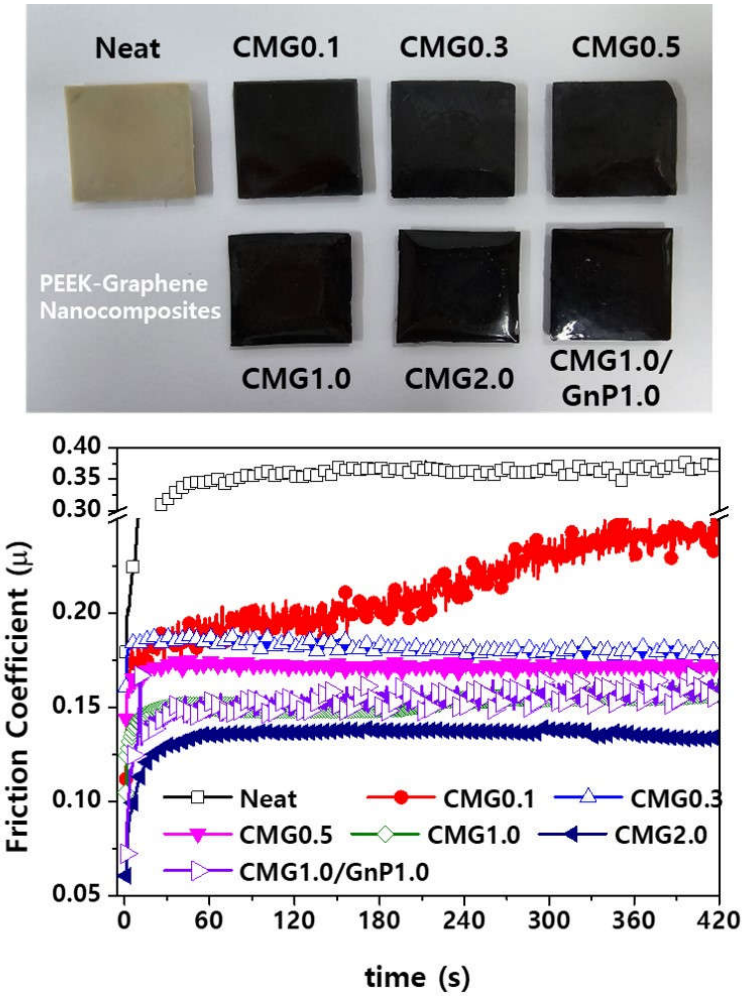


**Figure 12.** Friction coefficients of PEEK–graphene nanocomposites for various graphene contents.

3.2.4. Electrical Properties

Electronic devices are vulnerable to electrostatic discharge, which is generated by frictional electrification during manufacturing, handling, packaging, and transportation. Electrostatic discharge can severely damage electronic equipment [17]. To mitigate electrostatic discharge, protective packaging with low electrical resistance is essential to prevent charge accumulation and facilitate charge flow [26]. Electrically insulating materials typically exhibit a relatively high surface resistance of at least $10^{11}$ ohm/sq, hindering the flow of electrons across the surface. In contrast, materials with antistatic and dissipative properties exhibit an intermediate electrical resistance of $10^{4}$–$10^{8}$ ohm/sq, which allows for electrical conduction [17,18]. Figure 13 shows the surface resistance of the PEEK–graphene nanocomposites as a function of graphene content. Pristine PEEK is an electrically insulating polymer, and its surface resistance exceeds the measurement range of the surface resistance meter used in this study. Hence, its surface resistance is $10^{14}$ ohm/sq or higher. Graphene was used to reduce the surface resistance of the PEEK–graphene nanocomposites. As shown in Figure 13, the CMG0.1 sample does not exhibit a decrease in the surface resistance. However, CMG0.3 exhibits significantly reduced surface resistance in the range of $10^{11}$–$10^{12}$ ohm/sq. The surface resistance of the nanocomposites gradually decreases with increasing concentrations of CMG+. At concentrations exceeding 1.0 wt.%, a further decrease is observed until reaching stability. As shown in Figure 13, the surface resistance of the CMG1.0/GnP1.0 sample is significantly lower than that of the CMG2.0 sample with the same graphene content. As confirmed by EA and Raman

 doi:10.20944/preprints202502.0159.v1



spectroscopy, the GnPs exhibit high crystallinity and purity. Hence, its electrical conductivity is higher than that of CMG+. However, to ensure that the nanocomposite exhibits adequate electrical performance, the additive required is higher than that of CMG+. This is because CMG+ is thicker with a single layer measuring 1–2 nm. The excellent electrical performance of the CMG1.0/GnP1.0 provides the most convincing evidence that the CMG in PEEK–graphene forms a strong 3D network through ionic bonding. GnPs are easily desorbed from the surface of a PEEK–graphene nanocomposite and dispersed freely into graphene sheets inside the nanocomposite to form an optimal electrical pathway.

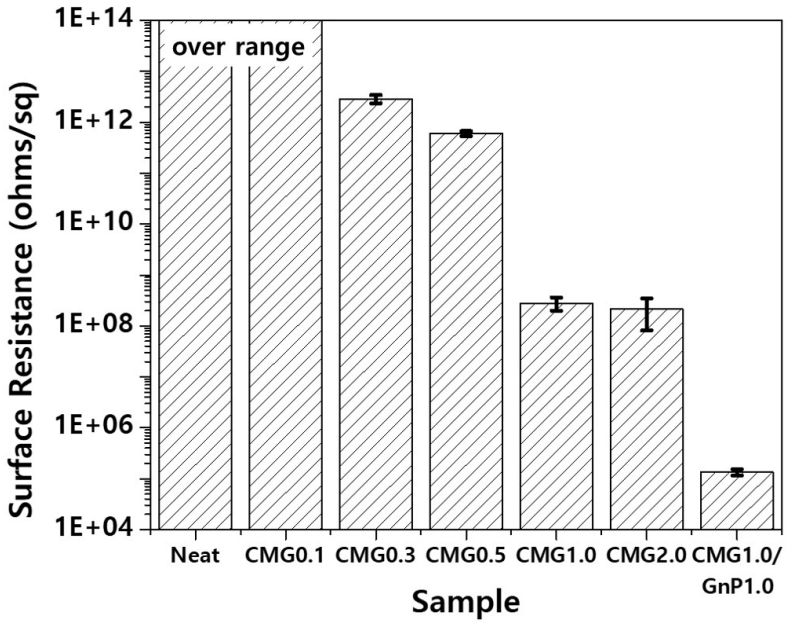


**Figure 13.** Surface resistance of PEEK–graphene nanocomposites for various graphene contents.

## 4. Conclusions

This study focused on enhancing the functionality of PEEK for semi-finished items. PEEK, which exhibits remarkable chemical resistance and thermal stability, is commonly used in the manufacturing of semiconductors and display devices. To protect these products, the PEEK must possess anti-static and fire-retardant properties. Furthermore, the wear particles formed by frictional abrasion can significantly impact product defects, underscoring the importance of their anti-wear characteristics. In this study, functionalized graphene was self-adsorbed onto the surface of a PEEK powder to produce nanocomposites. In PEEK–graphene nanocomposites, graphene hindered the diffusion of polymer chains, reducing the crystal size. In contrast, it improved the thermal stability of PEEK by impeding the movement of volatile decomposition products (barrier effect). In addition, graphene served as a solid lubricant, reducing the friction coefficient and surface resistance compared to pure PEEK. Graphene content of at least 1.0 wt.% was required to improve friction and electrical characteristics. However, the graphene content should be kept low considering the melt flow characteristics and size distribution. Therefore, an optimal adjustment of the graphene content in the nanocomposite is necessary to obtain the desired characteristics of the final product. The findings of this study are expected to enhance the utility of electrostatically dissipative PEEK. In future research, we plan to manufacture semi-finished products using PEEK–graphene nanocomposites and analyze their properties.

 doi:10.20944/preprints202502.0159.v1



**Supplementary Materials:** The following supporting information can be downloaded at the website of this paper posted on Preprints.org.

**Author Contributions:** Conceptualization, P.-C.L., S.H.H., and M.-G.K; methodology, S.H.H., J.H.K., and J.Y.S.; validation, Y.K.K., J.U.H., S.K.J., and B.-G.C.; formal analysis, S.H.H; investigation, J.H.K., Y.K.K, and J.U.H.; data curation, J.Y.S, Y.K.K.; writing—original draft preparation, S.H.H., P.-C.L. and M.-G.K.; writing—review and editing, P.-C.L, M.-G.K, and B.-G.C.; supervision, P. -C. L, M.-G. K, and B.- G. C. All authors read and agreed to the published version of the manuscript.

**Funding:** This work was supported by the Industrial Technology Innovation Program (20014475) funded by the Ministry of Trade, Industry, and Energy (MOTIE) of Korea.

**Data Availability Statement:** All data used during the study appear in the submitted article.

**Acknowledgments:** This work was supported by the Industrial Technology Innovation Program (20015819), and (20019105) funded by the Ministry of Trade, Industry, and Energy (MOTIE) of Korea.

**Conflicts of Interest:** The authors declare no conflict of interest. The funders had no role in the study design; collection, analyses, or interpretation of data; writing of the manuscript; or decision to publish the results.

## References

1. J.A. Puértolas, M. Castro, J.A. Morris, R. Ríos, A. Ansón-Casaos, Tribological and mechanical properties of graphene nanoplatelet/PEEK composites, Carbon. 2019;141:107–122.
2. M. Kalin, M. Zalaznik, S. Novak, Wear and friction behavior of poly-ether-ether-ketone (PEEK) filled with graphene, WS2 and CNT nanoparticles, Wear. 2015;855–862.
3. A.M. Díez-Pascual, M. Naffakh, C. Marco, G. Ellis, M.A. Gómez-Fatou, High-performance nanocomposites based on polyetherketones, Prog. Mater. Sci. 57 2012;57:1106–1190.
4. D.S. Bangarusampath, H. Ruckdäschel, V. Altstädt, J.K.W. Sandler, D. Garray, M.S.P. Shaffer, Rheology and properties of melt-processed poly(ether ether ketone)/multi-wall carbon nanotube composites, Polymer. 50 2009;50:5803–5811.
5. O. Coban, M. Ozgur Bora, E. Avcu, T. Sinmazcelik, The influence of annealing on the crystallization and tribological behavior of MWNT/PEEK nanocomposites, Polym. Compos. 2011;32:1766–1771.
6. A.M. Díez-Pascual, M. Naffakh, J.M. González-Domínguez, A. Ansón, Y. Martínez-Rubi, M.T. Martínez, B. Simard, M.A. Gómez, High performance PEEK/carbon nanotube composites compatibilized with polysulfones-II. Mechanical and electrical properties, Carbon. 2010;48:3500–3511.
7. M.C. Kuo, C.M. Tsai, J.C. Huang, M. Chen, PEEK composites reinforced by nano-sized SiO2 and Al2O3 particulates, Mater. Chem. Phys. 2005;90:185–195.
8. G. Zhang, H. Liao, H. Li, C. Mateus, J.M. Bordes, C. Coddet, On dry sliding friction and wear behaviour of PEEK and PEEK/SiC-composite coatings, Wear. 2006;260:594–600.
9. J.P. Davim, R. Cardoso, Effect of the reinforcement (carbon or glass fibres) on friction and wear behaviour of the PEEK against steel surface at long dry sliding, Wear. 2009;266:795–799.
10. R. Schroeder, F.W. Torres, C. Binder, A.N. Klein, J.D.B. de Mello, Failure mode in sliding wear of PEEK based composites, Wear. 2013;301:717–726.
11. H. Unal, U. Sen, A. Mimaroglu, Dry sliding wear characteristics of some industrial polymers against steel counterface, Tribol. Int. 2004;37:727–732.
12. J.P. Davim, N. Marques, Evaluation of tribological behavior of polymeric materials for hip prostheses application, Tribol. Lett. 2001;11:91–94.
13. D.L. Burris, W.G. Sawyer, A low friction and ultra low wear rate PEEK/PTFE composite, Wear. 2006;261:410–418.
14. H.B. Qiao, Q. Guo, A.G. Tian, G.L. Pan, L.B. Xu, A study on friction and wear characteristics of nanometer Al2O3 /PEEK composites under the dry sliding condition, Tribol. Int. 2007;40:105–110.
15. D. Puhan, J.S.S. Wong, Properties of polyetheretherketone (PEEK) transferred materials in a PEEK-steel contact, Tribol. Int. 2019;135:189–199.
16. M. Berer, Z. Major, G. Pinter, Elevated pitting wear of injection molded polyetheretherketone (PEEK) rolls, Wear. 2013;297:1052–1063.

 doi:10.20944/preprints202502.0159.v1



17. A. Pascual, M. Toma, P. Tostra, M.C. Grob, On the stability of PEEK for short processing cycles at high temperatures and oxygen-containing atmosphere, Polym, Degrad. Stabil. 2019;165:161–169.
18. S.-S. Yun, D.-H. Shin, K.-S. Jang, Influence of ionomer and cyanuric acid on antistatic, mechanical, thermal, and rheological properties of extruded carbon nanotube (CNT)/polyoxymethylene (POM) nanocomposites, Polymers. 2022;14:1849.
19. R.B. Rosner, Conductive materials for ESD applications: An overview, IEEE Trans. Device. Mater. Reliab. 2001;1: 9–16.
20. P.-C. Lee, S.Y. Kim, Y.K. Ko, J.U. Ha, S.K. Jeoung, D. Shin, J.H. Kim, M.-G. Kim, Tribological properties of polyamide 46/graphene nanocomposites, Polymers. 2022;14:1139.
21. A. Martínez-Gómez, S. Quiles-Díaz, P. Enrique-Jimenez, A. Flores, F. Ania, M.A. Gómez-Fatou, H.J. Salavagione, Searching for effective compatibilizing agents for the preparation of poly(ether ether ketone)/graphene nanocomposites with enhanced properties, Compos. A. 2018;113:180–188.
22. J.R. Potts, D.R. Dreyer, C.W. Bielawski, R.S. Ruoff, Graphene-based polymer nanocomposites, Polymer. 2011;52: 5–25.
23. D. Berman, A. Erdemir, A.V. Sumant, Graphene: A new emerging lubricant, Mater. Today. 2014;17:31–42.
24. B. Vasić, A. Matković, U. Ralević, M. Belić, R. Gajić, Nanoscale wear of graphene and wear protection by graphene, Carbon. 2017;120:137–144.
25. L. Sun, M. Cao, F. Xiao, J. Xu, Y. Chen, POSS functionalized graphene oxide nanosheets with multiple reaction sites improve the friction and wear properties of polyamide 6, Tribol. Int. 2021;154:106747.
26. Y. Mo, M. Yang, Z. Lu, F. Huang, Preparation and tribological performance of chemically modified reduced graphene oxide/polyacrylonitrile composites, Compos. A. 2013;54:153–158.
27. X.Y. Ye, X.H. Liu, Z.G. Yang, Z.F. Wang, H.G. Wang, J.Q. Wang, S.R. Yang, Tribological properties of fluorinated graphene reinforced polyimide composite coatings under different lubricated conditions, Compos. A. 2016;81:282–288.
28. D. Kang, S.H. Kim, D. Shin, J.T. Oh, M.-G. Kim, P.-C. Lee, Hygroscopic behavior of polypropylene nanocomposites filled with graphene functionalized by alkylated chains, Nanomaterials (Basel). 2022;12:4130.
29. P.-C. Lee, D. Kang, J.T. Oh, J.Y. Seo, D. Shin, J.-U. Jung, Y.K. Ko, J.U. Ha, M.-G. Kim, Reducing moisture absorption in polypropylene nanocomposites for automotive headlamps using hydrophobicity-modified graphene/montmorillonite, Nanomaterials (Basel). 2023;13:1439.